Bioorganic & Medicinal Chemistry Letters 22 (2012) 1989–1994

Contents lists available at SciVerse ScienceDirect

Bioorganic & Medicinal Chemistry Letters

journal homepage: www.elsevier.com/locate/bmcl

5-Aryl-4-carboxamide-1,3-oxazoles: Potent and selective GSK-3 inhibitors

Gabriella Gentile [a,*], Giancarlo Merlo [a,*], Alfonso Pozzan [b,*], Giovanni Bernasconi [a], Benjamin Bax [c], Paul Bamborough [c], Angela Bridges [c], Paul Carter [c], Margarete Neu [c], Gang Yao [c], Caroline Brough [c], Geoffrey Cutler [c], Aaron Coffin [c], Svetlana Belyanskaya [c]

[a] Department of Medicinal Chemistry, Neuroscience Centre of Excellence of Drug Discovery, GlaxoSmithKline, Via A Fleming 4, 37135 Verona, Italy
[b] Molecular Discovery Research, GlaxoSmithKline, Via A Fleming 4, 37135 Verona, Italy
[c] Molecular Discovery Research, GlaxoSmithKline, Gunnels Wood Road, Stevenage, Hertfordshire SG1 2NY, United Kingdom

ARTICLE INFO

Article history:
Received 9 December 2011
Revised 10 January 2012
Accepted 11 January 2012
Available online 21 January 2012

Keywords:
GSK-3 inhibitors
Glycogen synthase kinase-3 (GSK-3)
Bipolar disorder
Phenyloxazole carboxamide

ABSTRACT

5-Aryl-4-carboxamide-1,3-oxazoles are a novel, potent and selective series of GSK-3 inhibitors. The optimization of the series to yield compounds with cell activity and brain permeability is described.

Glycogen synthase kinase-3 (GSK-3), a multifunctional serine/threonine kinase existing as two isoforms (GSK-3α and GSK-3β) is a key regulator of numerous signalling pathways.[1] One function is to phosphorylate glycogen synthase (GS), implicating GSK-3 in type-2 diabetes.[2] In addition, GSK-3 inhibition is a therapeutic target for the treatment of neurodegenerative diseases such as Alzheimers,[3] and neurological diseases such as bipolar disorder.[4,5] Lithium is indicated as a preferential treatment for bipolar disorders, and the ability of this cation to inhibit GSK-3 has been proposed as a potential mechanism of action.[6] Due to this therapeutic potential, identification of GSK-3 inhibitors is a focus of research for both pharmaceutical companies and academic centres.[7] The availability of GSK-3β crystal structures[8,9] enables structure based lead discovery and optimization.

In our effort to discover novel GSK-3 inhibitors through affinity based screening of ultra-large DNA encoded libraries,[10] phenyloxazole carboxamide **1** was identified as a potent inhibitor of GSK-3 (Fig. 1). This represents a novel kinase inhibitor scaffold. However, one concern about compound **1** was its unfavourable physico-chemical properties, and potential low CNS permeability.[11–13] The polar surface area (PSA)[14,15] of CNS-penetrant molecules is usually ⩽60–70 Å^2, whilst that of compound **1** was 93 Å^2. To improve the CNS drug-like characteristics, analogues

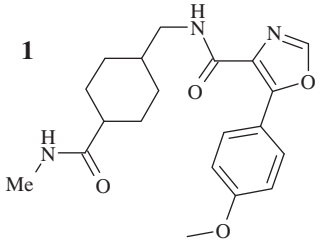

Figure 1. Hit **1**, pIC_{50} = 6.5 in the GSK-3β FP binding assay.[16]

were synthesised according to a general route (Scheme 1) which was used for all the compounds reported in this Letter.

Substituted carboxylic acids **2** were converted, directly or via acyl chloride formation, to phenyloxazole diethyl ester intermediates **3** by reaction with ethyl-isocyanoacetate. Hydrolysis to carboxylic acids **4** followed by amide coupling with appropriate primary amines led to the final compounds. Results are shown in Table 1.The *N*,*N*-dimethyl analogue **5** and the methylbenzamide **6** were of comparable potency to the hit **1**. Surprisingly, *N*-methylation led to the completely inactive *N*,*N*′-dimethylbenzamide **7**. This suggested that a hydrogen bond donor on the amide nitrogen next to the oxazole ring was essential for activity. The lower activity of the benzylamide **8** compared to **6** suggested that the hydrogen bond acceptor provided by the methylbenzamide group of **6** may be beneficial. Therefore, replacement of the benzamide with

* Corresponding authors. Tel.: +39 0458219355; fax: +39 0458218196 (G.G.).
E-mail addresses: gabriella.gentile@aptuit.com (G. Gentile), giancarlo.merlo@alice.it (G. Merlo), alfonso.pozzan@aptuit.com (A. Pozzan).

0960-894X/$ - see front matter Crown Copyright © 2012 Published by Elsevier Ltd. All rights reserved.
doi:10.1016/j.bmcl.2012.01.034

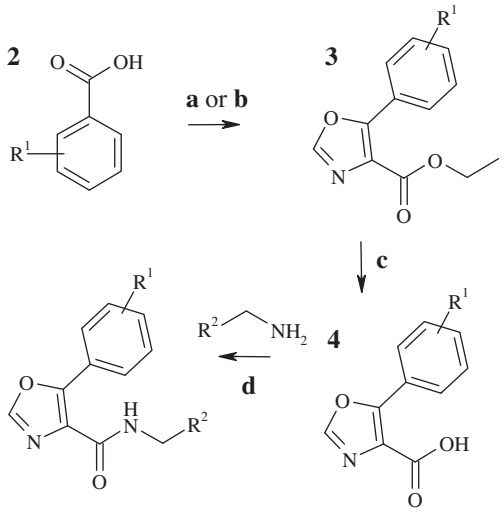

Scheme 1. General route to phenyl oxazole derivatives. Reagents and conditions: (a) (i) $SOCl_2$, reflux; (ii) ethyl isocyanoacetate, TEA, THF, rt; (b) ethyl isocyanoacetate, $(EtO)_2P(O)CN$, DIPEA, DMF, 0 °C to rt; (c) NaOH, EtOH, H_2O, rt; (d) HATU, DIPEA, DMF, rt.

hydrogen-bond containing heterocycles was attempted in order to improve upon **6** by reducing its polar surface area (PSA).

The pyridyl analogues **9**–**11** were prepared as analogues of **6** with reduced PSA. Gratifyingly, although the 2-pyridyl analogue **9** was 10-fold less active, compounds **10** and **11** showed similar activity to **6** (Table 1). Attempts to replace the methoxyphenyl ring of **11** with simple substituted phenyls in which the methoxy group was replaced or moved generally led to compounds with lower potency, for example, **12**–**16** (Table 1).

Compound **11** proved to be particularly interesting due to its favourable selectivity profile against a panel of protein kinases. From 17 kinases tested, all but one (AKT1, AKT2, ALK5, ASK1, AurA, EGFR, IKKβ, InsR, ITK, JNK1, LCK, PAK1, PDK1, ROCK1, SYK and VEGFR2) had IC_{50} greater than 10 μM. The one exception was CDK-2 (pIC_{50} = 6.1), which is not surprising since apart from GSK-3α this is one of the most closely related kinases to GSK-3β, sharing 35% sequence identity. Because of this encouraging selectivity and the lower PSA with predicted improvement in CNS-permeability over **1**, **11** was chosen as the starting point for further lead optimization.

The binding mode of compound **11** (Fig. 2) was determined from a 1.98 Å X-ray crystal structure.[17] The essential hydrogen-bonding interaction typically donated to inhibitors by the hinge

Table 1
GSK-3β FP binding activity of **5**–**16**. $pIC_{50} = -\log_{10}(IC_{50})$[16]

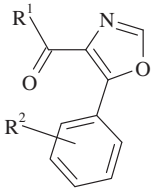

Compound	R^1	R^2	GSK-3β pIC_{50}	PSA (Å^2)
5	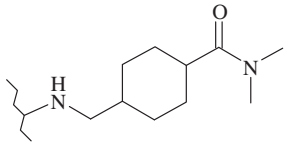	4-OMe	6.5	85
6	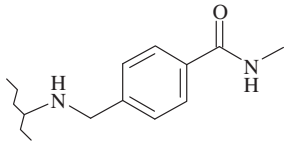	4-OMe	6.6	93
7	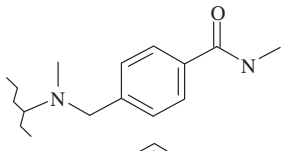	4-OMe	<4.6	85
8	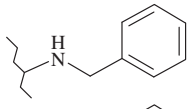	4-OMe	6.0	64
9	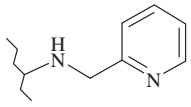	4-OMe	5.7	77
10	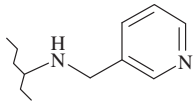	4-OMe	6.6	77

Table 1 (*continued*)

Compound	R^1	R^2	GSK-3β pIC_{50}	PSA (Å^2)
11	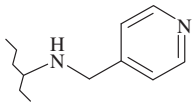	4-OMe	6.4	77
12	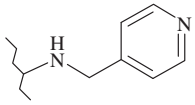	3-OH	6.2	88
13	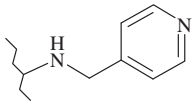	4-CF_3	5.2	68
14	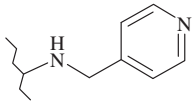	4-CN	5.5	92
15	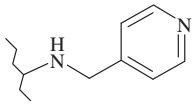	3-OMe	5.6	77
16	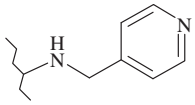	3-$CONH_2$	5.1	111

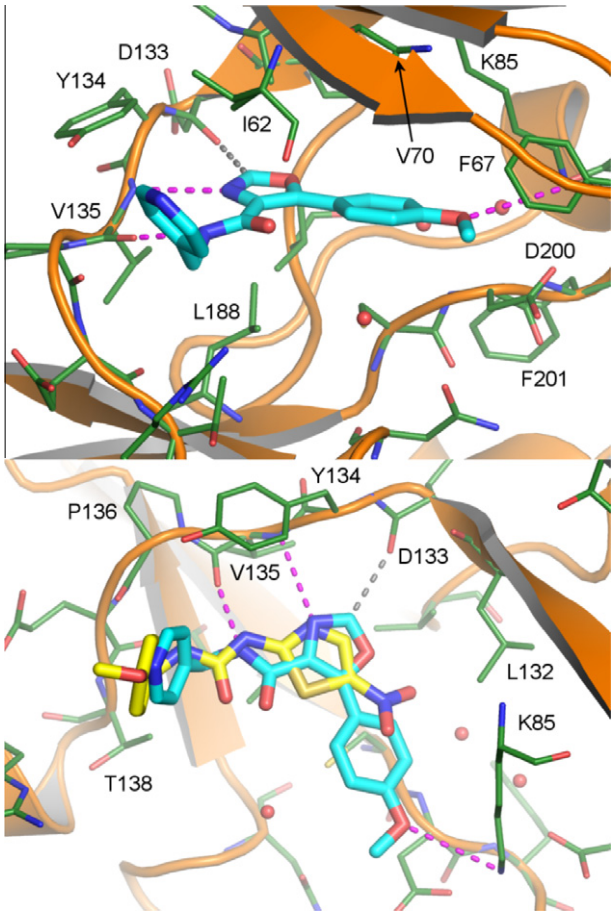

Figure 2. Top: X-ray structure of **11** in GSK-3β. Below: With AR-A014418 superimposed by protein coordinates (yellow).

(residue Val135 in GSK-3β) is accepted by the oxazole nitrogen atom. This interaction of the nitrogen of a monocyclic five-membered azole ring has been observed on other molecular scaffolds, for example in the 2-anilino 5-aryloxazole class of VEGFR2 kinase inhibitors.[18] The closest public GSK-3β crystal structure complex is with 5-nitro 2-urea thiazole AR-A014418, PDB code 1q5k.[19] The exact orientation of such hinge-binding rings is strongly influenced by the sterics of its substituents. In the above two examples the ligand atom adjacent to the acceptor nitrogen is substituted directly with an NH-R group, which donates a hydrogen bond to the hinge residue carbonyl (Val135). In contrast to this common substitution pattern, **11** has an unusual C(=O)NH-R group at this position, and it is this NH group that interacts with the carbonyl of Val135. This results in a rotation of the ring with respect to the typical binding mode exemplified by AR-A104418. As a consequence, the C-2 atom of the oxazole is in close proximity (2.9 Å) to the carbonyl of Asp133, acting as an unusual C–H hydrogen bond donor. The C-4 position amide substituent projects towards the solvent side of the site, in the region of Ile62, against which the pyridyl ring packs. The C-5-position phenyl substituent lies within the ATP-site in the vicinity of Val70, with the C-4 methoxy group in the region of the catalytic residues Lys85 and Asp200. Although reasonably close to the sidechain nitrogen of Lys85 (3.8 Å), the methoxy oxygen is not close enough to form a hydrogen bond, but it is possible that an electrostatic interaction contributes to the potency of **11**.

Two water molecules participate in a small buried network at the back of the site, interacting with the backbone NH atoms of Asp200 and Phe201 and the sidechain of Glu97. These are present in other complexes and can interact directly with ligands,[20] but in this case their closest interaction with **12** is edge-on to the methoxy-phenyl ring.

Based on the X-ray structural information it seemed that the interaction of the 4-methoxyphenyl with the pocket might be improved by optimising interactions with Phe67 and Val70. As the equivalent residue to Phe67 in CDK-2 is Tyr15, in principle this could also improve the selectivity. Because of this, an exploration of different substituents in the meta and para positions of the phenyl ring at the oxazole five-position was carried out following

Table 2
GSK-3β catalytic activity, cellular activity (CRMP-2), and CDK-2 activity of compounds **17–27**.[16]

	R^1		GSK-3β pIC_{50}	CRMP-2 pIC_{50}	CDK-2 pIC_{50}	PSA (Å^2)
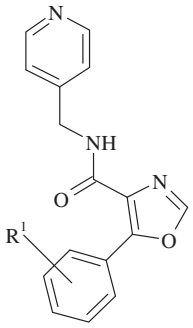	4-OMe	**11**	7.1	5.7	6.3	77
	3-Cl, 4-OMe	**17**	7.9	6.1	6.3	77
	3-F, 4-OMe	**18**	7.5	6.0	6.3	77
	2-F, 4-OMe	**19**	6.4	5.2	5.3	77
	2-Me, 4-OMe	**20**	5.5	⩽4.3	<4.8	77
	3-(4-Pyridyl), 4-OMe	**21**	5.9	4.4	<4.8	90
	3(4-Morpholinyl-4-OMe	**22**	5.7	4.5	<4.8	90
	3-Cl, 4-OPh	**23**	6.1	4.5	<4.8	77
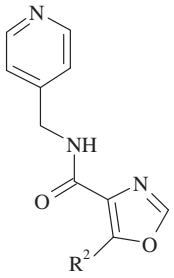	R^2					
	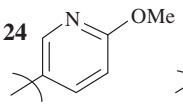	**24**	7.1	5.7	5.3	90
	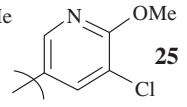	**25**	7.2	5.7	5.3	90
	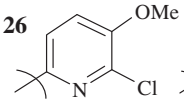	**26**	6.4	5.5	<4.8	90
	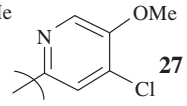	**27**	5.0	4.2	<4.8	90

Table 3
GSK-3β catalytic activity, cellular activity (CRMP-2), and CDK-2 activity of compounds **28–35**[16]

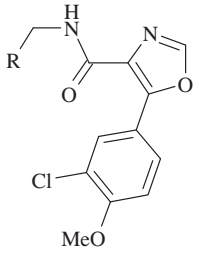

	R	GSK-3β pIC_{50}	CRMP-2 pIC_{50}	CDK-2 pIC_{50}	PSA (Å^2)
17	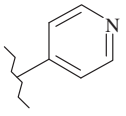	7.9	6.1	6.3	77
28	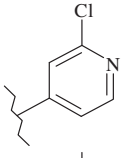	7.7	5.3	6.2	77
29	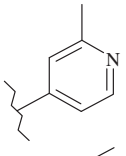	7.5	5.6	5.9	77
30	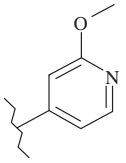	7.5	5.2	6.2	86

Table 3 (*continued*)

	R	GSK-3β pIC_{50}	CRMP-2 pIC_{50}	CDK-2 pIC_{50}	PSA (Å^2)
31	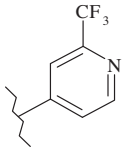	7.0	5.3	5.7	77
32	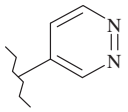	7.7	6.2	6.3	90
33	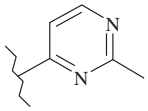	7.4	5.7	5.5	90
34	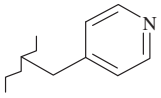	7.7	5.7	5.5	77
35	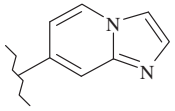	8.3	6.2	6.3	82

the synthetic route of Scheme 1. To overcome the tight-binding limit of the FP assay, these compounds were evaluated using a GSK-3β AlphaLISA assay and a cellular phospho-CRMP-2 assay (Table 2).[16]

The most potent compounds were those in which the methoxy at the phenyl C-4 position was accompanied by halogen groups at the C-3 position. For instance, the 3-chloro analogue **17** was best, closely followed by the 3-fluoro derivative **18**. Compared to **11** both showed significant improvements in GSK-3β potency, cellular activity, and CDK-2 selectivity. The beneficial halogen effect was strongly position-dependent: for example, the 2-fluoro analogue **19** was 10-fold less potent than the 3-fluoro compound **18**. The 2-methyl derivative **20** proved to be almost inactive, possibly because of disruption of the planarity in the aryl-oxazole system due to steric hindrance.

Compounds with larger groups at the C-3 position were also prepared (e.g., **21**, **22**) but these also had lower activity. The addition of a bulkier phenoxy group instead of the methoxy at the C-4 position was also unfavourable (**23**).

We next investigated substitution of the phenyl ring at the oxazole C-5 position with heterocyclic rings, preserving the position of the methoxy group at the C-4 position relative to the oxazole. Introduction of a pyridyl nitrogen at the 3-position relative to the attachment point was tolerated but modestly detrimental to GSK-3β activity (**24–25**), regardless of the presence of the chlorine substituent. Introduction of the pyridyl nitrogen adjacent to the oxazole substitution bond was unfavourable (**26**), even more so when it was placed on the opposite side of the ring to the chlorine (**27**).

Up to this point, **17** seemed to be the optimal compound for GSK-3β activity and PSA. We next returned to the oxazole C-4 position with further exploration of the heteroaromatic carboxamide while retaining the 3-chloro-4-methoxyphenyl moiety at the C-5 position. This was carried out by the route of Scheme 1. Decoration of the pyridine (**28–31**) and alternative heterocycles (**32–35**) were both attempted (Table 3). The 2-chloro, 2-methyl and 2-methoxy pyridyl compounds **28–30** were as potent as **17**, although the corresponding trifluoromethyl compound **31** was somewhat less active. The pyridazine **32** and methylpyrimidine **33** analogues also retained GSK-3β activity. Introducing a methylene spacer between the methyl-(4-pyridyl) moiety and the amide was tolerated and gave a small increase in CDK-2 selectivity (**34**). These findings suggested that a bulkier moiety at that position might increase potency, and indeed the imidazopyridine derivative **35** showed increased GSK-3β activity with respect to **17**.

Table 4
Rat pharmacokinetic parameters for compound **29** (iv dose 0.5 mg/kg, po dose 1 mg/kg)

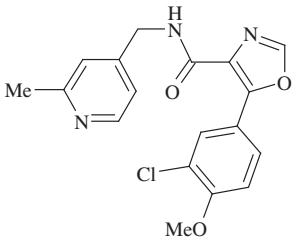

Clb (ml/min/Kg)	51
$t_{½}$ (h)	0.7
Vd (l/Kg)	2.4
F (%)	18
Brain/blood ratio	2.9

Compound **29** showed an acceptable profile in terms of activity, selectivity and PSA. This compound was selected as an exemplar of the 5-aryl-4-carboxamide-1,3-oxazole series for rat in vivo pharmacokinetic evaluation (Table 4).

The pharmacokinetic profile of **29** proved to be acceptable, with a low half life and volume of distribution, and moderate clearance and bioavailability. Brain penetration was good, validating the optimization strategy to reduce polar surface area.

In summary, optimization of the initial hit **1** led to the discovery of the novel 5-aryl-4-carboxamide-1,3-oxazoles series. Its binding mode has been elucidated by X-ray crystallography. Most of the exemplars showed good GSK-3β activity, cellular activity and a promising selectivity profile. Compound **29** proved to be brain penetrant, with a suitable pharmacokinetic profile for use in in vivo animal models.

References and notes

1. Cohen, P.; Frame, S. *Nat. Rev. Mol. Cell Biol.* **2001**, *2*, 769.
2. Nikoulina, S. E.; Ciaraldi, T. P.; Mudaliar, S.; Mohideen, P.; Carter, L.; Henry, R. R. *Diabetes* **2000**, *49*, 263.

3. Planel, E.; Sun, X.; Takashima, A. *Drug Dev. Res.* **2002**, *56*, 491.
4. Phiel, C. J.; Klein, P. S. *Annu. Rev. Pharmacol. Toxicol.* **2001**, *41*, 789.
5. Rowe, M. K.; Wiest, C.; Chuang, D. M. *Neurosci. Biobehav. Rev.* **2007**, *31*, 920.
6. Klein, P. S.; Melton, D. A. *Proc. Natl. Acad. Sci. U.S.A* **1996**, *93*, 8455.
7. Gentles, R. G.; Hu, S.; Dubowchik, G. M. *Annu. Rep. Med. Chem.* **2009**, *44*, 3.
8. Aoki, M.; Iwamoto-Sugai, M.; Sugiura, I.; Sasaki, C.; Hasegawa, T.; Okumura, C.; Sugio, S.; Kohno, T.; Matsuzaki, T. *Acta Crystallogr., Sect. D* **2000**, *56*, 1464.
9. Bax, B.; Carter, P. S.; Lewis, C.; Guy, A. R.; Bridges, A.; Tanner, R.; Pettman, G.; Mannix, C.; Culbert, A. A.; Brown, M. J.; Smith, D. G.; Reith, A. D. *Structure* **2001**, *9*, 1143.
10. Clark, M. A.; Acharya, R. A.; Arico-Muendel, C. C.; Belyanskaya, S. L.; Benjamin, D. R.; Carlson, N. R.; Centrella, P. A.; Chiu, C. H.; Creaser, S. P.; Cuozzo, J. W.; Davie, C. P.; Ding, Y.; Franklin, G. J.; Franzen, K. D.; Gefter, M. L.; Hale, S. P.; Hansen, N. J.; Israel, D. I.; Jiang, J.; Kavarana, M. J.; Kelley, M. S.; Kollmann, C. S.; Li, F.; Lind, K.; Mataruse, S.; Medeiros, P. F.; Messer, J. A.; Myers, P.; O'Keefe, H.; Oliff, M. C.; Rise, C. E.; Satz, A. L.; Skinner, S. R.; Svendsen, J. L.; Tang, L.; Van, V. K.; Wagner, R. W.; Yao, G.; Zhao, B.; Morgan, B. A.; Tang, L. *Nat. Chem. Biol.* **2009**, *5*, 647.
11. Kelder, J.; Grootenhuis, P. D.; Bayada, D. M.; Delbressine, L. P.; Ploemen, J. P. *Pharm. Res.* **1999**, *16*, 1514.
12. Van der Waterbeemd, H.; Camenish, G.; Folkers, G.; Chretien, J. R.; Raevsky, O. A. *J. Drug Target* **1998**, *6*, 151.
13. Leeson, P. D.; Davis, A. M. *J. Med. Chem.* **2004**, *47*, 6338.
14. Ertl, P.; Rohde, B.; Selzer, P. *J. Med. Chem.* **2000**, *43*, 3714.
15. Pajouhesh, H.; Lenz, G. R. *NeuroRx* **2005**, *2*, 541.
16. The GSK-3 FP and AlphaLISA assays, the CDK-2 Leadseeker assay and the cellular CRMP-2 AlphaLISA assay were performed as described in Ref. 19. CRMP-2 (Collapsin Response Mediator Protein-2) is a GSK-3b substrate.
17. Truncated GSK-3b (27–393) was co expressed with FRATtide (197–226) by dual baculovirus infection of Sf-9 cells (using a MOI of 3 for each virus), the protein was purified as described in Ref. 8 and co-crystals grown with compound as described in Ref. 19. Data to 1.98 Å were collected from a single frozen crystal on beam-line ID-23-1 at the European synchrotron radiation facility (ESRF). The crystal structure of compound **11** in complex with GSK-3β and FRATtide was refined from another structure determined in the same cell (from pdb code: 1gng) and deposited in the pdb with code 4afj.
18. Harris, P. A.; Cheung, M.; Hunter, R. N., III; Brown, M. L.; Veal, J. M.; Nolte, R. T.; Wang, L.; Liu, W.; Crosby, R. M.; Johnson, J. H.; Epperly, A. H.; Kumar, R.; Luttrell, D. K.; Stafford, J. A. *J. Med. Chem.* **2005**, *48*, 1610.
19. Bhat, R.; Xue, Y.; Berg, S.; Hellberg, S.; Ormo, M.; Nilsson, Y.; Radesater, A. C.; Jerning, E.; Markgren, P. O.; Borgegard, T.; Nylof, M.; Gimenez-Cassina, A.; Hernandez, F.; Lucas, J. J.; Diaz-Nido, J.; Avila, J. *J. Biol. Chem.* **2003**, *278*, 45937.
20. Gentile, G.; Bernasconi, G.; Pozzan, A.; Merlo, G.; Marzorati, P.; Bamborough, P.; Bax, B.; Bridges, A.; Brough, C.; Carter, P.; Cutler, G.; Neu, M.; Takada, M. *Bioorg. Med. Chem. Lett.* **2011**, *21*, 4823.